*31st EPS Conference on Plasma Phys. London, 28 June - 2 July 2004 ECA Vol.**28G**, P-4.183 (2004)*

First experiments in NBI Heated Plasmas in the TJ-II stellarator

M. Liniers, C. Alejaldre, J. Alonso, M.A. Acedo, L. Almoguera, F. de Aragón, E. Ascasíbar, A. Baciero, R. Balbín, E. Blanco, B. Brañas, E. Calderón, A. Cappa, R. Carrasco, F. Castejón, J.R. Cepero, A.A. Chmyga[(1)], J. Doncel, N.B Dreval [(1)], S. Eguilior, L. Eliseev[(2)], T. Estrada, A. Fernández, J.M. Fontdecaba[(5)], C. Fuentes, A. García, I. García-Cortés, J. Guasp, J. Herranz, A. Hidalgo, C. Hidalgo, J.A. Jiménez, I. Kirpitchev, S.M. Khrebtov[(1)], A. Komarov[(1)], A.S. Kozachok[(1)], L. Krupnik[(1)], F. Lapayese, D. López-Bruna, A. López-Fraguas, J. López-Razola, A López-Sánchez, E. de la Luna, G. Marcon, R. Martín, M. Medrano, A.V.Melnikov[(2)], P. Méndez, K. J. McCarthy, F. Medina, B. van Milligen, I.S. Nedzelskiy[(3)], M. Ochando, P. Ortiz, J. L. de Pablos, L. Pacios, I. Pastor, M.A. Pedrosa, A. de la Peña, A. Petrov[(4)], S. Petrov[(6)], A. Portas, D. Rapisarda, J. Romero, L. Rodríguez-Rodrigo, A. Salas, E. Sánchez, E. Sánchez, J. Sánchez, M. Sánchez, K. Sarksian[(4)], C. Silva[(3)], N. Skvortsova[(4)], F. L.Tabarés, D. Tafalla, V. Tribaldos, J. Vega, G. Wolfers, B. Zurro

Laboratorio Nacional de Fusión. EURATOM-CIEMAT, 28040 Madrid, Spain
[(1)] Institute of Plasma Physics, NSC KIPT, 310108 Kharkov, Ukraine
[(2)] Institute of Nuclear Fusion, RRC Kurchatov Institute, Moscow, Russia
[(3)] Associação EURATOM/IST, Centro de Fusão Nuclear, 1049-001 Lisboa, Portugal
[(4)] General Physics Institute, Russian Academy of Sciences, Moscow, Russia
[(5)] Universitat Politècnica de Catalunya, Barcelona, Spain
[(6)] A.F. Ioffe Physical-Technical Institute, 194021, St.Petersburg, Russia

Introduction

First experiments with Neutral Beam Injection (NBI) heated plasmas have been performed in the TJ-II stellarator [1]. Beams of 400 kW port-through (H^0) power at 28 kV, are injected onto target plasmas created using one or two ECRH lines (200–400 kW).

Evidence of the first beam heated plasmas was recognized at the rebound of the soft X rays signal, usually a signature of a finite electron temperature, after an initial fall at ECRH cut off. A clear difference between ECH and NBI plasmas was observed with the Thomson scattering profiles. The first NBI maintained plasmas were often terminated in a thermal collapse. Different combinations of gas puffing, ECH heating and wall conditioning strategies have been investigated with the aim of optimizing the power coupling and density control at NBI plasmas. We have finally been able to maintain NBI plasma discharges with reasonable density control of up to 130 ms duration.

First NBI Plasmas

Thomson scattering profiles obtained along the evolution of the plasma from ECH to NBI heating are shown in Figure 1. The electron density profiles show a gradual evolution from the hollow shape typical of ECH plasmas with on-axis microwave injection to bell-shaped profiles at the NBI phase. The central density increases from 1.7 x 10^{19} m^{-3} at ECH cut off, up to 4.0 x 10^{19} m^{-3} near the end of the discharge. The steep electron temperature profiles of ECH plasmas are suddenly flattened at density cut-off, the central value changing from 1 keV to 200-300 eV.

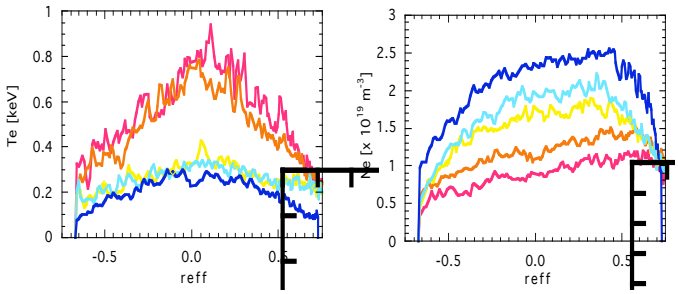

Figure 1: Evolution of TS profiles; a) T_e, b) n_e

When the NBI injection is combined with on-axis ECH heating, the rise in density above cut-off usually proceeds in a fast, uncontrolled way. A typical density waveform of such heating scenario is represented by the blue curve in Figure 2 (top). Plasma radiation diagnostics allow us to reject a sudden increase of Z_{eff} as the cause for the fast density rise. Spectroscopic measurements show no sharp increase of medium or high Z impurities. On the other hand, Langmuir probes measurements of turbulent transport at the plasma edge show a strong reduction in ExB turbulence as the NBI regime sets in [2]. Figure 2 (top) shows the particle flux waveform at an effective radius 0.95. It can be seen that the radial ExB turbulence induced flux is reduced by a factor 10 in the NBI regime. The sharp change of turbulent transport coincides with a significant increase in the ratio between density and particle recycling (H_α) as shown in Figure 2. Several modes below 300 kHz have been found in the frequency spectra of magnetic pick-up coils in the NBI regime. Edge density profiles obtained with Lithium beams show that the SOL density decay length decreases to half its ECRH value. The tails in density

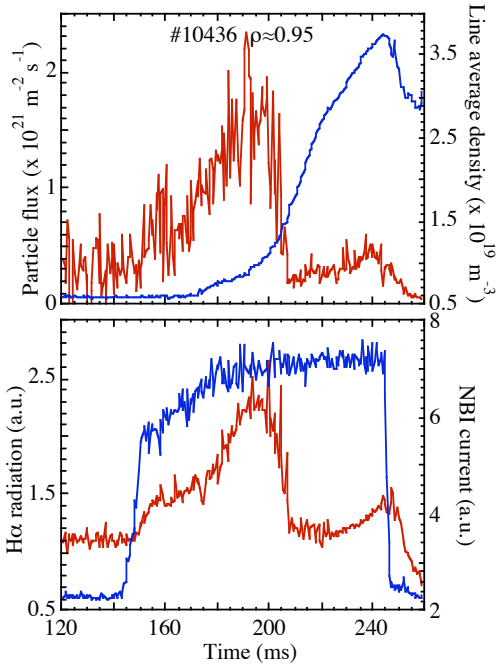

Figure 2: turbulent transport and Hα

profiles, normally observed in the SOL region in ECRH plasmas, disappear in the NBI phase. This picture of the plasma behaviour points in the direction of an improved confinement regime.

The behaviour of the plasma ions and impurities has also been studied at the transition between ECH and NBI regimes. The ion temperature as measured by a Neutral Particle Analyzer shows non-Maxwellian spectra with a first slope that evolves from 90 eV under ECH to around 130 eV under NBI. Impurity temperature and rotation are monitored using passive emission spectroscopy [3]. Toroidal rotation of impurities such as CV is seen to change drastically at NBI onset: the absolute value of the toroidal velocity decreases by a factor 4, although the negative (counter) sign is not reversed.

Computer simulations of the beam-plasma interaction with the Monte-Carlo code FAFNER combined with the transport code PROCTR allow us to calculate NBI absorption, fuelling, and plasma electric field. The selfconsistent ambipolar radial electric field resulting from PROCTR is always negative with NBI, while for ECHR discharges it is positive near the axis. Preliminary measurements of plasma potential with the Heavy Ion beam diagnostic [4] confirm the evolution of the electric field from positive at ECH plasmas to near sign reversal at the NBI regime. In Figure 3, plasma potential profiles at three successive discharge moments are shown: in the profile corresponding to a NBI maintained plasma, the slopes are negative, albeit small.

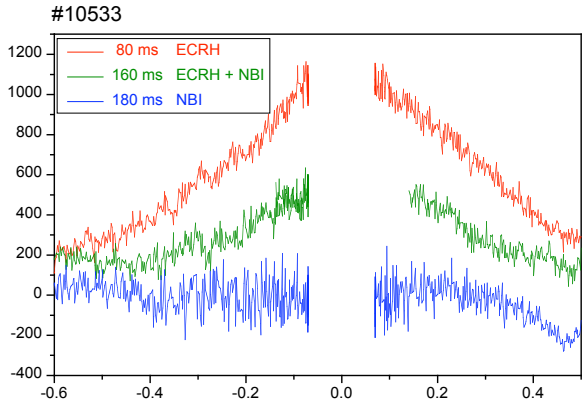

Fig 3: Profiles of plasma potential (V) by HIBP

Finally, as the plasma approaches the highest NBI densities ($4x10^{19}$ m^{-3}) an increase in the level of fluctuations and ExB transport has been systematically observed. Since these densities fall within the stellarator density limit scaling law, the finding can be interpreted as the increasing of edge transport near the density limit of TJ-II. Experimental results suggest the importance of both radiative and edge transport mechanisms in the physics of the density limit of TJ-II.

Comparison of different ECH-NBI scenarios

Density control in NBI discharges with a plasma target created by on-axis ECH has proven difficult. Repeated wall cleaning seems to help only to the extent of smoothing the density

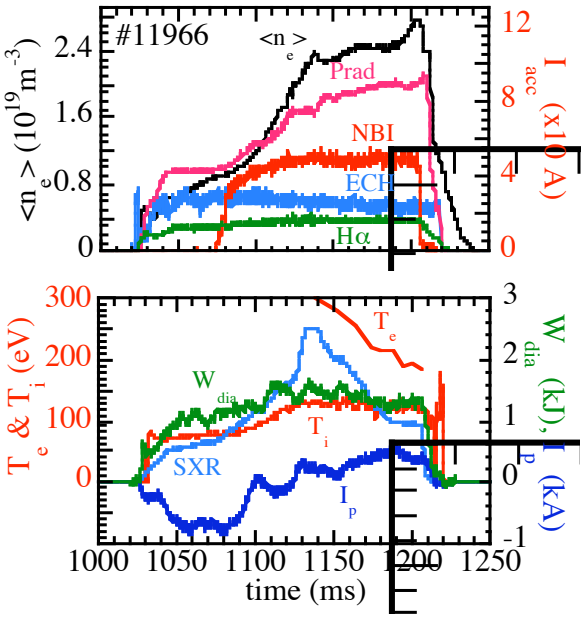

Figure 4: Time evolution of a NBI+ECH off-axis plasma discharge.

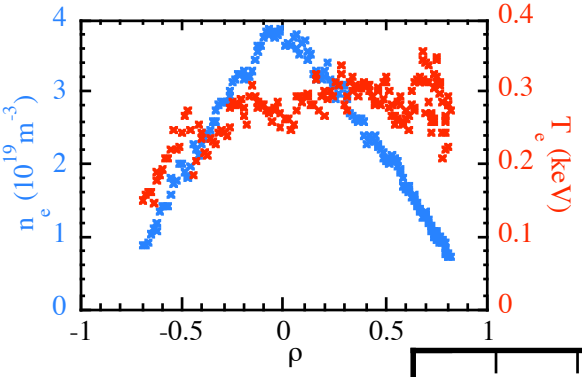

Figure 5: TS profiles of a NBI+ECH off-axis discharge.

rise, although there appears no sign of stabilizing its value. On the contrary, target plasmas created by off-axis ECH, maintained during the NBI phase, show promising. Figure 4 presents the time evolution of a discharge of that kind: the density is stable above cut-off until the end of the pulse. Electron temperature as monitored by the soft X ray signal is seen to rebound after an initial slide at cut-off. The ion temperature has a clear step up at NBI regime onset. Plasma radiation as monitored by the bolometers is in check. The plasma current reverses sign and the diamagnetic energy shows an appreciable increase. Such a distinctive behaviour is underlined by a comparison of Thomson scattering profiles: figure 5 shows that NBI + ECH off-axis plasmas have peaked density profile and flat temperature profile, as opposed to the NBI only case represented in figure 1.

The turbulent behaviour of both types of plasmas also differs. The MHD coherent modes appear in both cases, but the drastic reduction in the broadband spectrum occurs only at ECH removal in the on-axis case. A similar behaviour is observed with the Langmuir probes and the turbulence detected with the reflectometer: the turbulent spectra of the off-axis case is appreciably broader.

References

[1] M. Liniers *et al., Fusion Technology 1998 , **1**, 307*
[2] E. Calderón *et al., this Conference*
[3] B. Zurro *et al., this Conference*
[4] L. Krupnik *et al., this Conference*